

Photonic properties of erbium doped InGaN alloys grown on Si (001) substrates

I. W. Feng,¹ X. K. Cao,¹ J. Li,¹ J. Y. Lin,¹ H. X. Jiang,^{1,a)} N. Sawaki,² Y. Honda,³ T. Tanikawa,³ and J. M. Zavada⁴

¹Department of Electrical and Computer Engineering, Texas Tech University, Lubbock, Texas 79409, USA

²Department of Electrical and Electronic Engineering, Aichi Institute of Technology, Toyota 470-0392, Japan

³Department of Electronics and Akasaki Research Center, Nagoya University, Nagoya 464-8603, Japan

⁴Department of Electrical and Computer Engineering, Polytechnic Institute of New York University, Brooklyn, New York 11201, USA

(Received 13 January 2011; accepted 31 January 2011; published online 22 February 2011)

Erbium doped InGaN alloys (InGaN:Er) were grown on Si (001) substrates using metal organic chemical vapor deposition. The growth of epitaxial films was accomplished by depositing InGaN:Er on GaN templates deposited on 7.3° off-oriented Si (001) substrates which were prepared by etching and subsequent selective area growth. X-ray diffraction measurements confirmed the formation of wurtzite InGaN (1 $\bar{1}$ 01) epilayers, which exhibit strong photoluminescence emission at 1.54 μm . The observed emission intensity at 1.54 μm was comparable to that from similar alloys grown on GaN/AlN/Al₂O₃ templates. These results indicate the high potential for on-chip integration of erbium based photonic devices with complementary metal oxide semiconductor technology. © 2011 American Institute of Physics. [doi:10.1063/1.3556678]

Er-doped III-nitride semiconductors is a promising candidate for applications in optical communication.^{1,2} An Er³⁺ ion has an allowable intra-4*f* shell transition from its first excited state (⁴I_{13/2}) to the ground state (⁴I_{15/2}) and the transition corresponds to a wavelength of minimum optical loss in silica based optic fibers (1.5 μm). Additionally, Er-doped III-nitrides possesses larger bandgap energies which contributed to lower thermal quenching of 1.54 μm emission in comparison to other host semiconductors, such as GaAs, InGaP, and Si.³⁻⁷ Therefore, considerable efforts have been devoted into the development of photonic devices working at 1.54 μm based on Er-doped III-nitride materials (III-N:Er).¹ Recently, we have demonstrated heterogeneously integrated 1.54 μm emitters based on GaN:Er and p-i-n light emitting diodes based on InGaN:Er.^{1,8,9} These results opened up possibilities to fabricate electrically pumped optical amplifiers that possess the advantages of both semiconductor amplifiers (small size, electrical pumping, ability for photonic integration, etc.) and Er-doped fiber amplifiers (minimal crosstalk between different wavelength channels in wavelength-division multiplexing optical networks).

While Si has been the predominant material for microelectronics, the lack of a direct bandgap has restricted its use for photonics. However, advances in the development of Si optical waveguides and modulators have demonstrated the feasibility of Si photonics for optical communication devices applications. Nevertheless, since Si is not a suitable material to fabricate light emitters and optical amplifiers, compact infrared emitters on Si chips are highly desirable.¹⁰⁻¹⁵ In this paper, we report the attainment of strong 1.54 μm emission from InGaN:Er epilayers grown on 7.3° off-oriented Si (001) substrates. The crystalline and optical properties of InGaN:Er epilayers grown on various other templates are also presented. The results point to the possibility of combining Er-doped III-N optical devices with complementary metal oxide

semiconductor (CMOS) technology for applications in Si photonics.¹⁰⁻¹⁵

The InGaN:Er epilayers were simultaneously grown by metal organic chemical vapor deposition on four different templates [GaN/AlN/Si (001), GaN/AlN/Si (111), GaN/AlN/Al₂O₃ and Si (001)]. However, no epitaxial growth of single crystal InGaN was detected from the InGaN:Er samples grown directly on Si (001) substrates. Trimethylgallium, trimethylindium, tris-isopropylcyclopentadienylerbium, and ammonia (NH₃) were used as group-III and group-V precursors carried into the reactor by N₂ gas. Growth temperature of InGaN:Er alloys was ~760 °C. Due to the low vapor pressure of the metal organic Er source, the growth pressure had to be decreased to about 100 torr. Under this low growth pressure, the surface energy of InGaN (1 $\bar{1}$ 01) facet is comparatively high, which results in a relatively less stable growth surface and hence a slower growth rate than InGaN (0001).¹⁶ Indium (In) contents of InGaN:Er epilayers were verified by the peak positions of θ -2 θ scans in x-ray diffraction (XRD) measurement.¹⁷

Growth of III-nitrides on Si (001) substrates is challenging because of the different crystalline structures. To suppress dislocations and cracks in III-nitride epilayers grown on Si (001) substrates caused by the large mismatches of lattice and thermal expansion coefficient,¹⁸ we used selective area growth (SAG) and epitaxial lateral overgrowth (ELO) techniques to prepare GaN/AlN/Si (001) templates.¹⁹⁻²¹ As indicated by the schematic in Fig. 1(a), the periodic lined grooves with the sidewalls of Si (111) and Si ($\bar{1}\bar{1}$ 1) facets were obtained by selectively etching from 7.3° off-oriented Si (001) substrate by KOH chemical solution, and Si ($\bar{1}\bar{1}$ 1) facets were then coated with SiO₂ protective films to limit the III-nitride growth only along Si \langle 111 \rangle direction. An AlN intermediate layer of 70 nm was first grown on the patterned Si (001) substrate, and followed by the deposition of c-GaN alloy along Si \langle 111 \rangle direction until the overgrown layers

^{a)}Electronic mail: hx.jiang@ttu.edu.

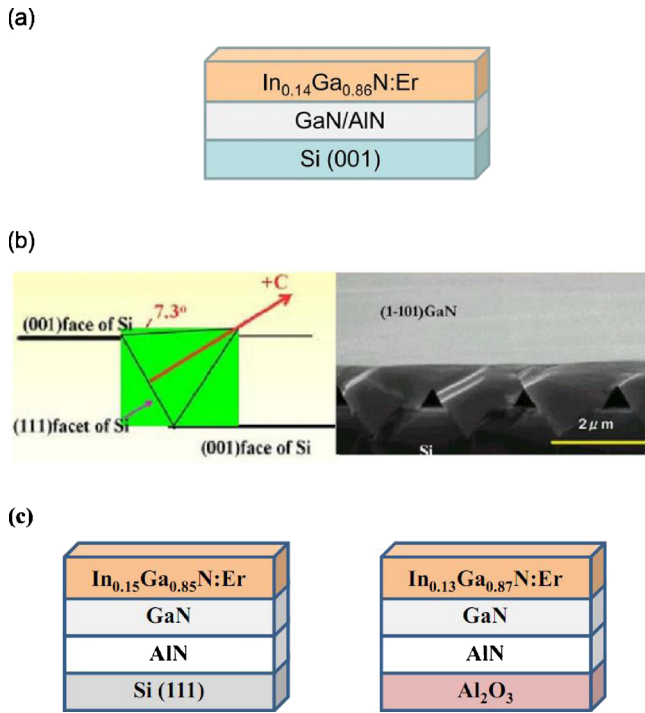


FIG. 1. (Color online) (a) Schematic of GaN/AlN/Si (001) template, (b) cross-sectional SEM image of a GaN/AlN/Si (001) template obtained by SAG and ELO, and (c) schematic of the multilayer structures of InGaN alloys grown on Si (111) and Al_2O_3 substrates.

were merged and the surface became smooth, as shown in the cross-sectional scanning electron microscope (SEM) image, Fig. 1(b). Growth using SAG and ELO techniques not only reduced the difference in thermal expansion coefficient by rotating the direction of c-GaN growth but also limited the propagation of dislocations. Smooth, crack-free GaN ($1\bar{1}01$) films were formed parallel to Si (001) substrate with a root mean square roughness $\sim 0.5\ \text{nm}$, obtained in $(10 \times 10)\ \mu\text{m}^2$ image size probed by atomic force microscopy.^{19–21} For comparison, GaN/AlN/Si (111) and GaN/AlN/ Al_2O_3 templates were also prepared by depositing the epitaxial layers directly on respective substrates, as illustrated in Fig. 1(c). θ - 2θ XRD spectra measured from these templates are shown in Fig. 2. While GaN (002) peaks were detected at 34.54° and 34.56° from GaN/AlN/Si (111) and GaN/AlN/ Al_2O_3 , respectively, the GaN ($1\bar{1}01$) peak at 36.80° was measured from the GaN/AlN/Si (001). For the GaN/AlN/Si (111) template, the shifted GaN (002) peak from the 2θ diffraction peak of strain-free c-GaN at 34.57° also implied a stronger tensile stress in c-direction (and compressive stress in a-plane). In contrast, by using ELO growth, the strain of the overgrown semipolar GaN ($1\bar{1}01$) on the patterned Si (001) substrate was relatively relaxed.

Photoluminescence (PL) spectra were measured at room temperature with above bandgap excitation ($\lambda_{\text{exc}} \sim 266\ \text{nm}$), which has been demonstrated to be more efficient than below bandgap excitation.⁴ PL spectra, focused mainly on $1.54\ \mu\text{m}$ emission, were used to characterize the optical properties of InGaN:Er epilayers grown on various templates. No PL signal was detected in InGaN:Er films grown directly on Si (001) substrate. In contrast, as shown in Fig. 3, $1.54\ \mu\text{m}$ emission was obtained from the InGaN:Er epilayer grown on the SAG GaN/AlN/Si (001) template, and its intensity at

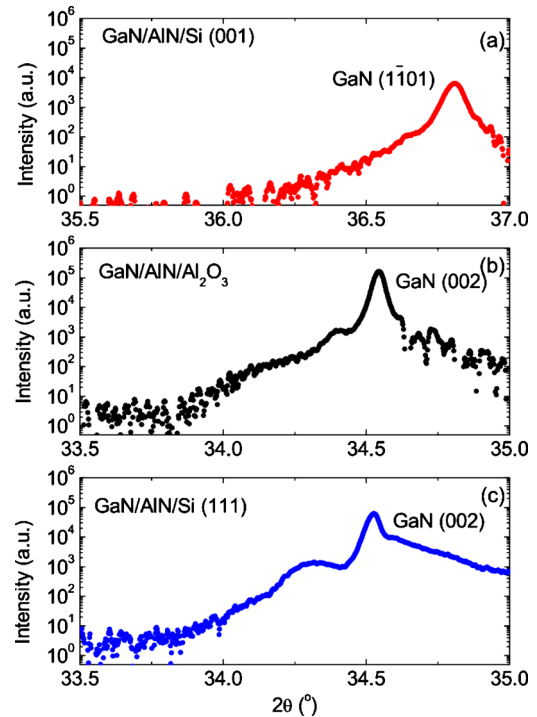


FIG. 2. (Color online) θ - 2θ XRD spectra detected from different templates used for Er doped InGaN growth: (a) GaN/AlN/Si (001), (b) GaN/AlN/ Al_2O_3 , and (c) GaN/AlN/Si (111).

$1.54\ \mu\text{m}$ was comparable to that of the InGaN:Er alloy grown on Al_2O_3 substrate. The intensity of $1.54\ \mu\text{m}$ emission obtained from InGaN:Er sample grown on GaN/AlN/Si (111) template was found to be up to five times stronger than that obtained from the other templates. The strong $1.54\ \mu\text{m}$ emission from the InGaN:Er/GaN/AlN/Si (111) sample corroborated to our previous results of GaN:Er grown on various substrates.²² The stronger emission may be partially re-

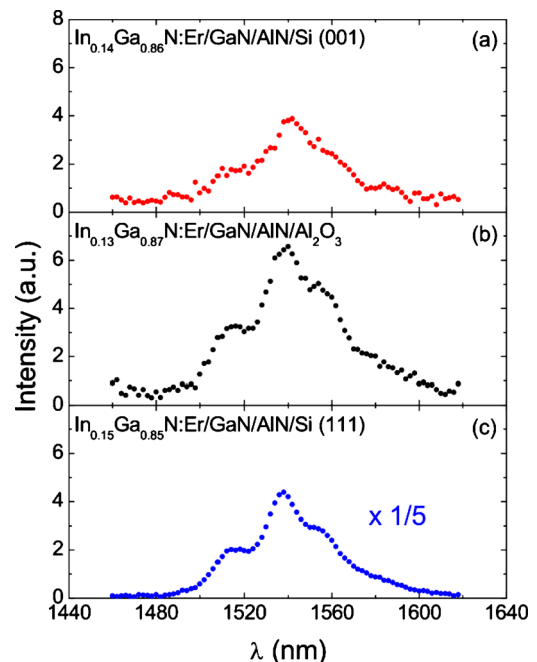


FIG. 3. (Color online) Room temperature infrared PL emission spectra near $1.54\ \mu\text{m}$ measured from $\text{In}_{0.14}\text{Ga}_{0.86}\text{N}:\text{Er}$ grown on different templates: (a) $\text{In}_{0.14}\text{Ga}_{0.86}\text{N}:\text{Er}/\text{GaN}/\text{AlN}/\text{Si}$ (001), (b) $\text{In}_{0.13}\text{Ga}_{0.87}\text{N}:\text{Er}/\text{GaN}/\text{AlN}/\text{Al}_2\text{O}_3$, and (c) $\text{In}_{0.15}\text{Ga}_{0.85}\text{N}:\text{Er}/\text{GaN}/\text{AlN}/\text{Si}$ (111).

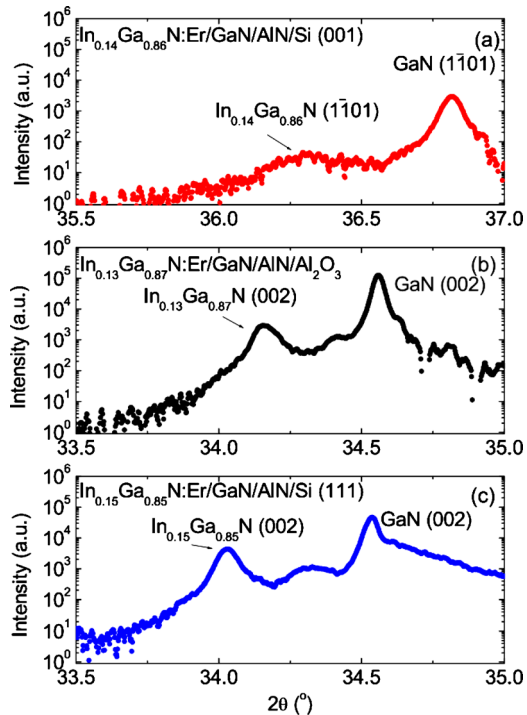


FIG. 4. (Color online) θ - 2θ XRD spectra measured from $\text{In}_{0.14}\text{Ga}_{0.86}\text{N}:\text{Er}$ grown on different templates: (a) $\text{In}_{0.14}\text{Ga}_{0.86}\text{N}:\text{Er}/\text{GaN}/\text{AlN}/\text{Si}(001)$, (b) $\text{In}_{0.13}\text{Ga}_{0.87}\text{N}:\text{Er}/\text{GaN}/\text{AlN}/\text{Al}_2\text{O}_3$, and (c) $\text{In}_{0.15}\text{Ga}_{0.85}\text{N}:\text{Er}/\text{GaN}/\text{AlN}/\text{Si}(111)$.

lated to the larger strain caused by the lattice mismatch between $\text{InGaN}:\text{Er}$ and $\text{Si}(111)$ substrates. The crystal electric field, attributed to the strain or stress, increases the asymmetry of the atomic configuration around Er^{3+} atoms so that the transition probability of the partially allowed intra- $4f$ transitions by the selection rule is enhanced. $\text{InGaN}:\text{Er}$ alloys grown on the strain-relaxed $\text{GaN}/\text{AlN}/\text{Si}(001)$ templates may be under a smaller strain, which results in less efficient intra- $4f$ transitions than in $\text{InGaN}:\text{Er}/\text{GaN}/\text{AlN}/\text{Si}(111)$ sample.

Figure 4 shows θ - 2θ XRD spectra of these $\text{InGaN}:\text{Er}$ samples, except for $\text{InGaN}:\text{Er}$ grown directly on $\text{Si}(001)$ substrate from which no XRD signal was detected. The wurtzite $\text{In}_{0.14}\text{Ga}_{0.86}\text{N}$ ($1\bar{1}01$) facet was measured from $\text{InGaN}:\text{Er}/\text{GaN}/\text{AlN}/\text{Si}(001)$ sample with a 2θ peak at 36.29° . $\text{InGaN}(002)$ peaks were detected from the $\text{InGaN}:\text{Er}/\text{GaN}/\text{AlN}/\text{Si}(111)$ and $\text{InGaN}:\text{Er}/\text{GaN}/\text{AlN}/\text{Al}_2\text{O}_3$ samples at 34.04° ($\text{In}\% \sim 15\%$) and 34.16° ($\text{In}\% \sim 13\%$), respectively. A small difference in In contents between these three samples could be attributed to the non-uniform strain and In distribution or different growth rates. Under the same growth conditions, the growth of $\text{InGaN}(1\bar{1}01)$ facet was found to be two times slower than that of $\text{InGaN}(0001)$ facet. This reduced growth rate of $\text{InGaN}(1\bar{1}01)$ facet results in a thinner Er -doped $\text{InGaN}(1\bar{1}01)$ layer, which also attributed to the lower intensity of the $1.54 \mu\text{m}$ emission and XRD signal. Further improvement of $1.54 \mu\text{m}$ emission and crystalline properties of Er doped

III-nitrides grown on $\text{Si}(001)$ substrates is expected by optimizing the growth conditions of $\text{InGaN}:\text{Er}(1\bar{1}01)$ alloys since the growth of Er doped III-nitrides on $\text{Si}(001)$ substrates is still in the embryonic state.

In summary, we have demonstrated the feasibility of growing Er -doped InGaN on $\text{Si}(001)$ substrates. This demonstration opens up the possibility of integrating electrically pumped $1.54 \mu\text{m}$ optical devices with CMOS technology. The intensity of $1.54 \mu\text{m}$ emission achieved from this $\text{InGaN}:\text{Er}$ alloy was found to be as good as that grown on $\text{GaN}/\text{AlN}/\text{Al}_2\text{O}_3$ substrates. These achievements indicate the possibility of on-chip nitride optical components for applications in optical communications, computers, and other functional Si photonic devices.

This work is funded by NSF (Grant No. ECCS-0854619). The authors would like to thank Dr. Tommy Wong of U.S. Army International Technology Center—Pacific for the coordination of this U.S./Japan collaboration. H.X.J. and J.Y.L. are grateful to the AT&T Foundation for the support of Ed Whitacre and Linda Whitacre Endowed chairs. J.M.Z. acknowledges support from NSF under the IR/D program.

- ¹R. Dahal, J. Y. Lin, H. X. Jiang, and J. Zavada, *Topics in Applied Physics: Rare Earth Doped III-Nitrides for Optoelectronic and Spintronic Applications*, edited by K. O'Donnell and V. Dierolf (Springer, The Netherlands, 2010), pp. 115–157.
- ²R. Dahal, C. Ugolini, J. Y. Lin, H. X. Jiang, and J. M. Zavada, *Appl. Phys. Lett.* **95**, 111109 (2009).
- ³J. Palm, F. Gan, B. Zheng, J. Michel, and L. Kimerling, *Phys. Rev. B* **54**, 17603 (1996).
- ⁴C. Ugolini, N. Nepal, J. Y. Lin, H. X. Jiang, and J. M. Zavada, *Appl. Phys. Lett.* **89**, 151903 (2006).
- ⁵T. D. Culp, U. Hommerich, J. M. Redwing, T. F. Kuech, and K. L. Bray, *J. Appl. Phys.* **82**, 368 (1997).
- ⁶Y. Fujiwara, T. Ito, M. Ichida, T. Kawamoto, O. Watanabe, I. Yamakawa, A. Nakamura, and Y. Takeda, *Jpn. J. Appl. Phys., Part 1* **38**, 1008 (1999).
- ⁷C. Ugolini, N. Nepal, J. Y. Lin, H. X. Jiang, and J. Zavada, *Appl. Phys. Lett.* **90**, 051110 (2007).
- ⁸R. Dahal, C. Ugolini, J. Y. Lin, H. X. Jiang, and J. Zavada, *Appl. Phys. Lett.* **93**, 033502 (2008).
- ⁹R. Dahal, C. Ugolini, J. Y. Lin, H. X. Jiang, and J. Zavada, *Appl. Phys. Lett.* **97**, 141109 (2010).
- ¹⁰X. Liu, R. Osgood, Y. Vlasov, and W. Green, *Nat. Photonics* **4**, 557 (2010).
- ¹¹J. D. Liang, *Nat. Photonics* **4**, 511 (2010).
- ¹²G. T. Reed, *Nature (London)* **427**, 595 (2004).
- ¹³R. Soref, *Silicon* **2**, 1 (2010).
- ¹⁴G. Bona, R. Germann, and B. Offrein, *IBM J. Res. Dev.* **47**, 239 (2003).
- ¹⁵B. Jalali, *J. Lightwave Technol.* **24**, 4600 (2006).
- ¹⁶A. Zauner, F. Theije, P. Hageman, W. Enckevort, J. Schermer, and P. Larsen, *Temperature dependent morphology transition of GaN films*, MRS Symposia Proceedings No. 557 (Materials Research Society, Pittsburgh, 1999), p. 345.
- ¹⁷M. A. Moram and M. E. Vickers, *Rep. Prog. Phys.* **72**, 036502 (2009).
- ¹⁸S. Pal and C. Jacob, *Bull. Mater. Sci.* **27**, 501 (2004).
- ¹⁹T. Hikosaka, T. Narita, Y. Honda, M. Yamaguchi, and N. Sawaki, *Appl. Phys. Lett.* **84**, 4717 (2004).
- ²⁰Y. Honda, N. Kameshiro, M. Yamaguchi, and N. Sawaki, *J. Cryst. Growth* **242**, 82 (2002).
- ²¹Y. Honda, Y. Kawaguchi, Y. Ohtake, S. Tanaka, M. Yamaguchi, and N. Sawaki, *J. Cryst. Growth* **230**, 346 (2001).
- ²²I. W. Feng, J. Li, A. Sedhain, J. Y. Lin, H. X. Jiang, and J. Zavada, *Appl. Phys. Lett.* **96**, 031908 (2010).